The Tokamak Physics Experiment*

Ronald C. Davidson† and Robert J. Goldston
Princeton Plasma Physics Laboratory, Princeton, New Jersey 08543

George H. Neilson
Oak Ridge National Laboratory, Oak Ridge, Tennessee 37831

Keith I. Thomassen
Lawrence Livermore National Laboratory, Livermore, California 94550

(Received 14 November 1994; accepted 13 February 1995)

The mission of the Tokamak Physics Experiment (TPX) [Nevins *et al.*, *Plasma Physics and Controlled Nuclear Fusion*, Würzburg (International Atomic Energy Agency, Vienna, 1992), Vol. 3, p. 279] is to develop the scientific basis for an economically competitive and continuously operating tokamak fusion power source. This complements the primary mission of the International Thermonuclear Experimental Reactor (ITER) [ITER Document Ser. No. 18 (International Atomic Energy Agency, Vienna, 1991)], the demonstration of ignition and long-pulse burn, and the integration of nuclear technologies. The TPX program is focused on making the demonstration power plant that follows ITER as compact and attractive as possible, and on permitting ITER to achieve its ultimate goal of steady-state operation. This mission of TPX requires the development of steady-state regimes with high beta, good confinement, and a high fraction of a self-driven bootstrap current. These regimes must be compatible with plasma stability, strong heat-flux dispersion in the divertor region, and effective particle control. © *1995 American Institute of Physics.*

I. INTRODUCTION

Motivated by design studies of tokamak-based fusion power plants that indicate how to achieve potential reductions in the cost of electrical power,[1,2] and stimulated by a growing experimental and theoretical basis that supports the ideas on which the essential improvements are based,[3–6] there is an increased worldwide interest in the advanced tokamak. A centerpiece in the Department of Energy's fusion program is the Tokamak Physics Experiment (TPX),[7] while an advanced tokamak thrust is also being discussed with the Japan Tokamak-60 Super Upgrade (JT-60SU) design proposal.[8] Both of these devices rely on advanced tokamak modes of operation in regimes with a high bootstrap current fraction, which is necessary for efficient (or high-power gain) power plant operation.

The TPX tokamak is being designed by a national team of scientists and engineers from universities, national laboratories, and industry. The conceptual design of TPX has been completed, and industrial contractors have now been selected to begin the detailed design, research and development, and hardware fabrication for major subsystems. The research program on TPX will be performed by a multi-institutional national research team, and will demonstrate the physics basis for continuously operating power plants with a lower cost than those based on "standard" rather than "advanced" physics regimes. The elements of these advanced regimes, and the machine features required for such operation, are described in Sec. II, and the theoretical and experimental basis for advanced tokamaks and the TPX physics design are summarized in Secs. III and IV, respectively.

*Paper 8I2, Bull. Am. Phys. Soc. **39**, 1749 (1994).
†Invited speaker for the National TPX Team.

II. ADVANCED TOKAMAK FEATURES

Increasing the power density per unit of volume by operating close to (and increasing) the limiting values of plasma beta $\beta=2\mu_0\langle p\rangle/B^2$ is a promising approach to improved power plant economics, because this generally provides the largest-power output for a given capital investment. Here B is the toroidal magnetic field, and we make use of the fact that the power density is proportional to the square of the pressure p. Another important improvement for economical tokamak power plants is continuous operation, because of the cost penalties associated with pulsed operation.[9]

To operate in a continuous mode, the plasma current I_p must be driven noninductively by radio-frequency waves or ion beams, a too-inefficient technique, unless most of the current is carried by the internally generated bootstrap current. High bootstrap current fractions $f_{\rm bs}\sim\sqrt{\epsilon}\beta_p$ favor operation at high poloidal beta $\beta_p=2\mu_0\langle p\rangle/B_p^2$. Here, $\epsilon=a/R=A^{-1}$ is the inverse aspect ratio, where a and R are the minor and major radii, respectively, of the plasma.

We introduce the normalized beta β_N defined by $\beta_N=\beta/(I_p/aB)$, and define $\xi=(1+\kappa^2)^{1/2}\sqrt{2}$, where κ is the elongation and $\sqrt{\xi}B_p = \mu_0 I_p/2\pi a$. This gives $\beta\beta_p=(5\xi\beta_N)^2$, showing for prescribed values of ξ and β_N that an increase in β_p requires a decrease in β. The ratio β/β_p can be expressed as

$$\frac{\beta}{\beta_p}=\left(\frac{I_p}{5aB\xi}\right)^2=\left(\frac{\xi}{q^*A}\right)^2, \tag{1}$$

so that decreasing the normalized current I_p/aB increases the ratio β_p/β. The parameter $q^*=(2\pi a^2\xi^2 B)/\mu_0 I_p R$ is approximately equal to the edge safety factor, and should not exceed the range 4–6 for good power plant economics. Evidently, higher aspect ratio also leads to a higher ratio of

β_p/β, although the optimum aspect ratio for an advanced tokamak reactor remains uncertain and requires a larger database.

Several features of steady-state operation are apparent from these relationships. First, the current must be lowered (relative to inductive operation) to increase β_p relative to β, and second, to restore higher β for more power output it is advantageous to increase β_N beyond the conventional Troyon limit of ~ 3 for first stability operations. Operating within the first stability regime one can nonetheless find attractive modes of operation, such as that developed in Advanced Reactor Innovative Evaluation Studies (ARIES),[1] the ARIES-I mode, which has $q_0 \approx 1.3$ (where q_0 is the safety factor on axis), a relatively flat, monotonic $q(r)$ profile, and a β_N of 3. To reach second stable operation (for ballooning modes) requires $q_0\beta_N \gg 3$ and $\epsilon\beta_p \sim 1$, the latter being consistent with high bootstrap current operation. The reversed-shear mode,[6] having an inversion of the $q(r)$ profile and a relatively high central $q_0 (q_0 \sim 3)$, typically reaches second stability in the core, has a β_N of 5 with a close-fitting wall, and is one of the more attractive advanced tokamak modes, owing to its good magnetohydrodynamic (MHD) stability and reduced transport in the core.[10,11]

From power plant system studies,[1] there is nearly a factor of 2 difference in the cost of electricity between 1000 MW electric (MWe) power plants that are pulsed and have values of $\beta_N \approx 2.5$, compared with those operating continuously at $\beta_N \approx 5$, most of the difference being due to the increased β_N. Thus, a key requirement for advanced tokamaks is a configuration with pressure exceeding the conventional Troyon limit on MHD stability. Necessary features may include conducting walls for kink-mode stabilization, plasma rotation to make the resistive walls behave as though they were ideal, coils for fast feedback control of plasma position and control of helical modes, and plasma profile controls to provide access to the second-stability regime.

An optimum steady-state power plant will likely have lower current than a pulsed power plant with the same power output. Because the plasma energy confinement is proportional to current, the ability to operate with enhanced confinement $H>2$, where $H=\tau_E/(\tau_E)^L$ is the enhancement factor, τ_E is the energy confinement time, and $(\tau_E)^L$ is the conventional low-mode confinement time, is especially important for steady-state tokamaks. Values of H up to 4 have been achieved experimentally in short-pulse operation, and such values are more than adequate for optimized tokamak power plants, which require $H \sim 3$ for plants in the 750 MWe range, and $H<2$ for plants in the 1500–2000 MWe range.

Besides the stability controls discussed above, two design features are especially critical for achieving improved performance (i.e., for raising H and β_N). The first is strong plasma cross-section shaping. In particular, the triangularity δ, and also the elongation κ, should be made relatively high through the proper design of the poloidal field system. The second critical design feature is a current-profile control system. The current profile shape affects performance, and control is necessary to correct any mismatch between the profile of the internally generated bootstrap current and that required for high-β_N stability and enhanced confinement. Control can be provided through an appropriate combination of auxiliary current-drive systems, and, to a lesser extent, through appropriate fueling sources and plasma exhaust systems. Both central current drive (e.g., from neutral beam injection and fast ion cyclotron waves), and off-axis current drive (e.g., from lower hybrid or electron cyclotron waves) are required.

These advanced tokamak features are reflected in the specific design characteristics of TPX described later in this paper. In addition, because TPX has superconducting poloidal and toroidal field coils, the device is inherently capable of steady-state operation, though it is initially limited to 1000 s operation by its auxiliary systems. All relevant physical processes are expected to come into equilibrium on that time scale.

TPX is designed to test the physics of continuous advanced tokamak operation, and will address several related issues critical to the success of the International Thermonuclear Experimental Reactor (ITER)[12] and future tokamak power plants. These include operation with steady-state divertors, fueling, and particle exhaust systems; plasma control in steady state; diagnostics and data acquisition in steady-state operation; and internal remote maintenance (the annual deuterium–deuterium neutron fluence in TPX will be high). And perhaps, most importantly, TPX integrates both the physics and technology for continuous advanced tokamak operation in a single device for the first time in the tokamak development program.

III. THEORETICAL AND EXPERIMENTAL BASIS FOR TPX

The physics basis for an advanced tokamak power plant, and for the Tokamak Physics Experiment, has developed rapidly in the past few years. Areas of special importance include MHD stability, current drive, and divertor physics. Results in these three areas will need to be integrated in advanced tokamak operating modes in TPX, in later phases of ITER, and eventually in a fusion demonstration power plant.

A. Magnetohydrodynamic stability

In the area of ideal magnetohydrodynamic (MHD) stability, theoretical calculations have shown that attractive MHD-stable operating modes exist for steady-state tokamak reactors. In the absence of an ideally conducting wall, values of normalized beta $\beta_N \sim 3.0$ can be achieved in configurations with $q_0 \sim 1.3$, and about 75% bootstrap current at $R/a = 4-4.5$ and $q_{95} \sim 4$, as shown in the Advanced Reactor Innovative Evaluation Studies-I (ARIES-I)[13] and in the Steady-State Tokamak Reactor (SSTR)[14] study. With a conducting wall located at an effective radius of $1.3a$, a second scenario with β_N in the range of 5–6 can be achieved through the use of a "reversed-shear" configuration[6,15] (Fig. 1). This configuration can have as much as 95% bootstrap current, with good alignment between the bootstrap current and total current profiles. The value of q_{95} at which this is achieved, depends on aspect ratio, increasing with decreasing R/a. At the TPX value of aspect ratio $R/a = 4.5$, which is optimized to permit the study of both scenarios and to widen the ex-

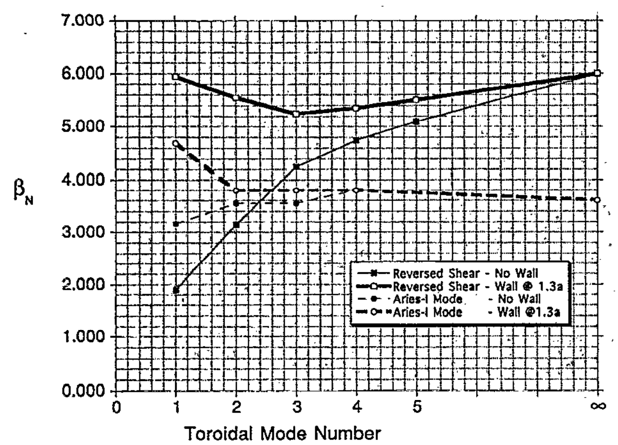

FIG. 1. Calculated ideal MHD stability for reversed shear mode (β_N=4.8, f_{bs} = 0.93) and for the ARIES-I mode (β_N=3.1, f_{bs}=0.68) with and without a conducting wall.

perimental database for a tokamak demonstration power plant, q_{95}~4 gives simultaneously high bootstrap-current fraction and high β.

In the ideal MHD plasma model one expects that a real conducting wall can only stabilize the external kink mode for a time scale of order the wall-penetration time for the helical mode of interest (τ_{wall}). Experimentally, however, it has been observed that the stability of rotating high-β plasmas in the Princeton Beta Experiment-Modification (PBX-M)[16] and the DIII-D tokamak,[17] which persist for times much longer than τ_{wall}, are best fit with MHD models, which treat the actual wall as ideal. A theoretical analysis,[18] including dissipative effects, suggest that rotation speeds about 1/20 of the Alfvén speed should result in stabilization. Experiments on DIII-D[19] indicate that even lower speeds, with ω_{rot} at the resonant surface, perhaps as low as $\sim 1/\tau_{wall}$ or $1/\tau_{res}$, may be sufficient. A very recent theoretical analysis finds similar results.[20] The Japan Fusion Tokamak Version 2 Modification (JFT-2M) has shown that it is possible to impart modest toroidal plasma rotation to a tokamak plasma using externally generated ac helical magnetic fields.[21] The issues of MHD control through passive stabilization, plasma rotation, and possibly feedback control on the slow τ_{wall} time scale, are important areas of continuing physics research and development.

B. Current drive and current profile control

In the area of current drive and current profile control, there has been good progress as well. The PBX-M tokamak has demonstrated that lower-hybrid-generated fast electrons are well confined to their birth flux surfaces in MHD-quiescent discharges, but can be diffused radially by MHD activity.[22] Experiments on the Japan Tokamak-60 Upgrade (JT-60U) have demonstrated both effective current drive at currents up to 3.5 MA, and also significant changes in the current profile associated with phase control, consistent with theory.[23] The DIII-D[24] and Tore Supra[25] tokamaks have begun to demonstrate the effectiveness of fast-wave current drive for on-axis seed-current generation. The Tokamak Fusion Test Reactor (TFTR) has demonstrated the ability to obtain off-axis electron heating via mode conversion in the ion cyclotron range of frequency, opening up the possibility of current profile control in this frequency range.[26] Similar possibilities may be present using the fast-wave/lower-hybrid current drive synergy mechanism discovered on the Joint European Torus (JET).[27] Neutral–beam current drive is a well-accepted tool whose flexibility for current profile control has been recently demonstrated in JT-60U.[23] Thus, the "tool kit" for current profile control on TPX—fast-wave current drive for on-axis "seed" current drive, lower hybrid current drive for off-axis current profile control, and neutral beam injection for bulk current drive—appears to be developing well, and may have the potential for more flexibility than originally anticipated. Key areas of ongoing physics research and development include steady-state antennas for the radio-frequency systems, and the understanding and optimization of their wave spectra to allow the highest possible efficiency and flexibility.

C. Divertor physics

The area of divertor physics has been very active as well. The TPX divertor design combines features from both the DIII-D advanced pumped divertor and the Alcator C-Mod[28] vertical-plate divertor. In the DIII-D advanced divertor geometry, neutrals generated at the separatrix strike point on the divertor plate are channeled into the pump volume, as in the TPX design. This provides for very effective pumping, and optimization of the possibility for impurity entrainment in the plasma flow.The experimentally confirmed ability of the DIII-D advanced divertor to pump out the particle inventory from the chamber walls at a rate of 35 Torr l/s,[29] even during a short plasma pulse, is very promising for the ability of TPX to achieve high-performance, low-wall-recycling modes of operation in a long pulse. Helium density measurements in DIII-D show no evidence of profile peaking relative to the electron density in the "Low" (L) mode, the ELMing "High" (H) mode (where ELM refers to edge-localized modes), the ELM-free H mode, and the "Very High" (VH) mode, suggesting that helium pumping should not be a special problem in any of these operating regimes.[30] The vertical-plate geometry, now being tested in Alcator C-Mod and in JET is also looking very promising. This divertor concept is based on the idea that neutrals generated at the strike points of field lines outside the separatrix are directed onto the highest-heat-flux separatrix field lines. The geometry is optimized to minimize the temperature and ultimately the pressure (for "detached" operation) at the separatrix strike point, the location where heat-flux reduction is most critical. Experimental observations in the Alcator C-Mod[31] and JET[32] have confirmed these predictions, increasing the confidence level in this design.

An important feature of the TPX configuration is its double-null geometry. The high triangularity required for high-performance operation (see below) results in short field-line lengths between the X point and the inner divertor. In the double-null configuration, the very low heat and particle flux along these field lines makes a flux-expanded divertor solution in this region acceptable. A high-triangularity

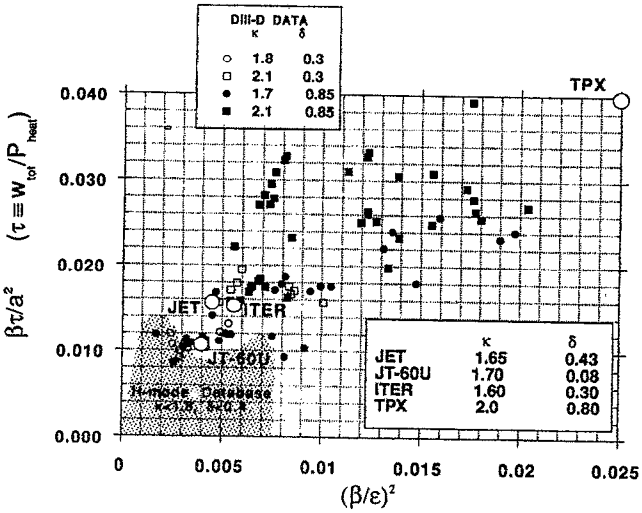

FIG. 2. Achieved values at $\beta\tau/a^2$ and $(\beta/\epsilon)^2$ for DIII-D VH-mode shape scan plotted against ITER H-mode database, and highest performance JET and JT-60U data. ITER and TPX target points included.

single-null configuration would provide too little volume for a slot divertor configuration on the inside in the major radius. Recent results from DIII-D[33] confirm the assumptions that in a double-null configuration the inner-wall heat flux is very small, and that the up–down heat-flux balance is relatively easy to obtain, even in cases with strong gas puffing, which reduces the peak divertor heat flux by a factor of 3 or more. United States reactor studies continue to favor the double-null configuration, using a radial-access maintenance scheme for the blanket and first wall.[9]

A key remaining area of divertor physics research and development is the demonstration of long-pulse operation with strong heat flux reduction at the divertor strike point, while retaining high-performance, moderate density, and good cleanliness in the main chamber. The recent feedback-controlled neon-puffing-and-pumping experiments in the Axially Symmetric Divertor Experiment Upgrade (ASDEX-U)[34] are encouraging in this regard, and should be extended to high-performance, ELM-free VH modes.

D. Advanced tokamak operating modes

No existing experimental facility can integrate all of the key features required for a full test of the optimal operating mode for a steady-state advanced tokamak. Indeed this is the mission of TPX. However, significant experimental progress has been made in demonstrating advanced tokamak operating modes at a moderate pulse length. Experiments on DIII-D and PBX-M have achieved values of $\beta\tau_E/a^2[\propto nT\tau_E/(aB)^2]$ and $(\beta/\epsilon)^2$ (proportional to fusion power density, since $B_0 \propto \epsilon^{-1/2}$ for fixed B_{coil}) approaching those required for TPX, but not in steady state, nor with large bootstrap current fractions. These results clearly show the importance of high triangularity for advanced performance (Fig. 2). Recent experiments on JET have also shown that the longest ELM-free high-performance plasmas are obtained at high triangularity.[35] In addition, JET has now sustained $\beta_N \geqslant 3$, $\beta_p \sim 1.7$, $H \sim 2$ for up to seven seconds.[36] The JT-60U tokamak has achieved discharges with about 0.6 s of fully noninductive operation, with 74% bootstrap fraction.[37]

TABLE I. TPX machine parameters.

	Baseline	Upgrade
Toroidal field, B (T)	4.0	
Plasma current, I_P (MA)	2.0	
Pulse length (s)	1000	$\geqslant$1000
Major radius, R (m)	2.25	
Minor radius, a (m)	0.50	
Aspect ratio, R/a	4.5	
Elongation, κ_x	2.0	
Triangularity, δ_x	0.8	
Neutral beam power, P_{NB}(MW)	8	24
ICRF power, P_{IC}(MW)	8	18
Lower hybrid power, P_{LH} (MW)	1.5	3.0

The attractiveness of the reversed-shear operating mode was first demonstrated experimentally in pellet enhanced performance (PEP) modes on JET.[4] This result has now been reproduced on Tore Supra,[38] where reversed (or very low) core shear has also been produced using lower hybrid current drive. This has resulted in low core transport coefficients and very high central electron temperatures. The DIII-D tokamak has observed dramatic improvements in core confinement with $q_0 > 1$.[39] On TFTR,[40] a new approach has been developed to access the reversed-shear regime, using neutral beams to "freeze in" a high core q value at low current, and then ramping the plasma current up to about 2 MA. Dramatically improved confinement is found in the reversed-shear core.[41]

The need for integration of advanced-tokamak modes, e.g., demonstration of wall-stabilized reversed-shear regimes, or stable sustainment of high bootstrap-fraction current profiles for long-pulse operation, awaits further experimental results from present machines and extension of these results on TPX. The physics research and development in this area shows encouraging progress toward this goal.

IV. PHYSICS DESIGN OF TPX

A. Tokamak configuration

The major parameters for the baseline TPX facility (i.e., as configured for its initial operation) are summarized in the "Baseline" column of Table I. A drawing of the tokamak cross section is displayed in Fig. 3. The tokamak is designed with no inherent limitations on pulse length, however, the baseline facility with ancillary systems provides a pulse length of 1000 s. This is ample for current-profile equilibration for several skin times (~100 s). Plasma–wall equilibration times are more difficult to predict, since they depend on details of the plasma–wall interface; it is not yet clear how the wall conditions will equilibrate in long-pulse operation with active pumping. The pulse length of TPX can be extended to test plasma reliability at the level of one disruption per 10 h by removing the limits imposed by external systems, such as cryopumping and cooling.

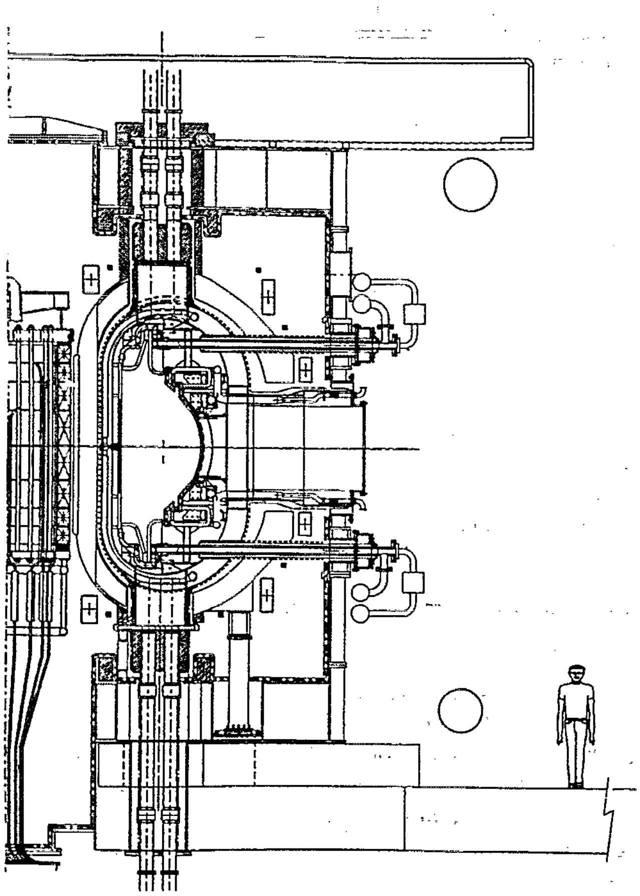

FIG. 3. Elevation of the TPX tokamak.

The TPX plasma cross section features a double-null poloidal divertor configuration with high elongation κ and high triangularity δ (values of these displayed in Table I are measured at the X point), the favored geometry for advanced plasma performance. The choice of the aspect ratio R/a ($=1/\epsilon$) of 4.5 is motivated by high-bootstrap reactor design points,[1,14] which establish the need to expand the tokamak physics database in the high-aspect-ratio regime.

The plasma and main components inside the vacuum vessel are shown in Fig. 4. As explained in Sec. III C, the double-null configuration permits an open configuration, which allows substantial variation in the inner separatrix position and hence plasma elongation. The outer divertor is arranged in a deep (0.57 m) slot configuration with a vertical target plate intersecting the magnetic surfaces at a shallow angle to maximize the surface area available for heat removal. This "reentrant" configuration encourages high recycling and divertor detachment. A central baffle plate in the private region helps gas (fuel plus any impurities) stay trapped near the outer target and improves particle exhaust by minimizing backstreaming from the pumping plenum. Further details of the divertor physics design are described in Ref. 42. A cylindrical inner limiter centered on the midplane protects the vacuum vessel from plasma losses and neutral–beam shinethrough. Toroidal limiters protect components between the inner limiter and inner divertor target. On the outside, toroidal limiters above and below the midplane and a set of discrete poloidal limiters protect the RF wave launchers. The toroidal limiters are attached to passive stabilizers, which are copper conducting structures used together with internal control coils to control plasma position and MHD modes. Carbon–fiber composite materials are used on all plasma-facing surfaces, both in the divertor and in the main chamber, and all use actively cooled heat sinks to handle the steady-state plasma heat loads.

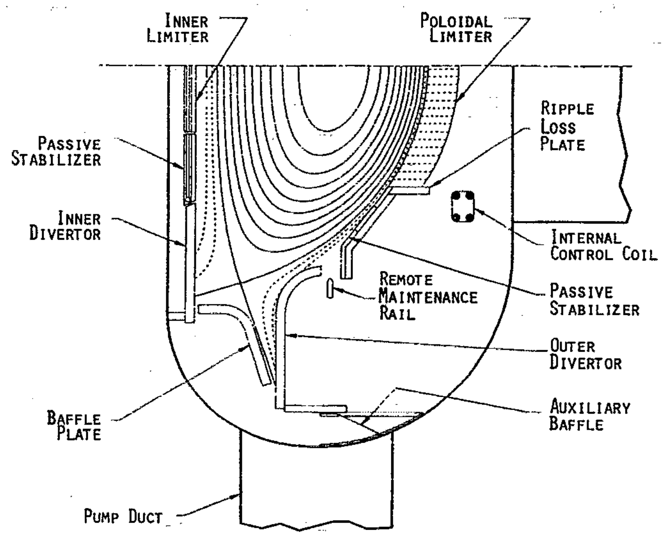

FIG. 4. Cross section of the TPX plasma magnetic surfaces below the midplane, inside (solid) and outside (dashed) the plasma's boundary separatrix. The dashed surfaces shown intersect the midplane 1 and 2 cm from the outboard boundary and at 2.5 and 5 cm from the inboard boundary. The main in-vessel components are shown and described in the text.

B. Heating and current drive systems

The TPX heating and current drive system[43] includes neutral beams and two radio-frequency (RF) systems: one in the ion cyclotron range of frequencies (ICRF) and the other in the lower hybrid (LH) range. The 120 keV neutral beams provide bulk current drive, ion heating, core fueling, toroidal momentum drive, and a signal source for key diagnostics. The 40–80 MHz ICRF system provides electron or ion heating and centrally peaked fast-wave current drive. The 3.7 GHz lower hybrid system provides off-axis current profile control, an efficient bulk current drive at low temperature, and electron heating. The initial plasma heating power from each of these systems is indicated in the "Baseline" column of Table I; a total of 17.5 MW is available. The power can be increased to the levels indicated in the "upgrade" column of Table I, to a total of 45 MW. Alternate upgrade heating configurations to accommodate electron cyclotron waves, ion Bernstein waves, and higher-energy neutral beams are possible as upgrades.

C. Diagnostics

The TPX will initially be configured with a basic diagnostic complement[44] necessary for machine operations and for characterization of advanced tokamak operating modes. Diagnostic capabilities for plasma control will be available, including measurements of the current profile. Diagnostics to measure plasma parameters in the core, edge, and divertor regions will be provided, and limited capability for studying fluctuations and fusion products will be included. The device has ample port space to accommodate diagnostic upgrades to provide expanded capabilities.

D. TPX operating modes

A zero-dimensional model based on ITER physics rules,[45] but extended to include a more accurate bootstrap current model[46] has been employed to determine power balance and current-drive requirements globally. Specified profiles of safety factor, density, and temperature are used to more accurately calculate the bootstrap current, fusion products, and volume-averaged quantities. The profiles used are based on those found to be stable in MHD studies. The baseline complement of heating systems is sufficient to sustain a configuration with $\beta_N=3.5$ (about the first-stability beta limit) in deuterium plasmas with a confinement enhancement factor H of about 3.4. Here a $A_i^{1/2}$ dependence in the confinement scaling is assumed, where A_i is the ion mass. The toroidal field can be reduced to 3 T for enhanced-beta studies: $\beta_N=4.2$ is attainable in this regime with $H=3$. Upgrades to the plasma heating and coil refrigeration systems will permit such studies to be extended to full magnetic field and significantly higher plasma performance. Further details of these zero-dimensional operating points are discussed in Ref. 47.

The Analyzer for Current Drive Consistent with MHD Equilibrium (ACCOME)[48] is the current-drive simulation code used to predict the current profiles attainable with the TPX heating systems. Models for the bootstrap current and for neutral–beam, fast-wave, and lower-hybrid current drive are included. The density and temperature profiles are specified with the help of the zero-dimensional model to ensure consistency with global power balance requirements. The ACCOME model is used to determine the current-profile control capabilities needed to realize profiles with ceratin desirable MHD stability characteristics, although the stability of the profiles actually predicted must be checked.

Table II summarizes two model operating modes of the baseline TPX, an ARIES-I, and a reversed-shear mode. While the full 17.5 MW is needed in both cases to satisfy power balance (based on the zero-dimensional model), less than 10% of the fast-wave power is needed for current profile control. In the ARIES-I case, a small fast-wave current is driven in the forward direction to obtain $q=1.3$ on axis. In the reversed-shear case, the fast-wave current is driven in the reverse direction and the lower hybrid current drive is critical in maintaining a negative-shear region out to $r/a\approx 0.8$. The current profiles and safety factor profiles for these cases are shown in Fig. 5; the stability has not been analyzed. These modeling studies show that the ability to vary the direction of the on-axis fast-wave current drive is important for control, even though only a small fraction of the available ICRF heating power may be used for this purpose. Lower hybrid current drive helps to control the profile in the outer half of the plasma, particularly when used to correct the mismatch between the bootstrap profile and a desired reversed-shear profile. The combination of three current drive systems and the variable phasing capabilities of the radio-frequency systems will provide flexibility for investigating a wide range of scenarios and accommodating uncertainties in the bootstrap current profiles.

TABLE II. Deuterium plasma operating modes with current profile control.

Operating mode	ARIES-I	Reverse shear
Toroidal field, B (T)	4.0	3.0
NBI power, $P_{\rm NB}$(MW) (CD/Htg)	8.0/8.0	8.0/8.0
ICRF power, $P_{\rm IC}$(MW) (CD/Htg)	0.6/8.0	0.8/8.0
LH power, $P_{\rm LH}$(MW) (CD/Htg)	1.5/1.5	1.5/1.5
LH normalized wave number, $n_\parallel$	2.25	2.50
H factor, τ_E/τ_L mode	3.1	3.3
$\langle n_e\rangle$ (10^{20} m^{-3})	0.75	0.67
$n_e(0)(10^{20}$ m$^{-3})$	1.00	0.90
T_{e0} (keV)	15	14
T_{i0} (keV)	15	14
β_N (% m T/MA)	3.6	5.1
$\epsilon\beta_p$	0.57	0.62
NBI-driven current (kA)	399	393
ICRF-driven current (kA)	63	−76
LH driven current (kA)	90	93
Bootstrap current (kA)	1218	1203
Total current, I_P, (kA)	1769	1613
Bootstrap fraction, $f_{\rm bs}$	0.69	0.75

E. Equilibrium control

The poloidal field system in TPX is designed to sustain full-current ($q_{95}\approx 3$) equilibria with β_N up to 5 and a range of current profile shapes corresponding to internal inductance parameter $l_i(3)$ values from 0.4 to 1.2. This flexibility will allow the stability limits of enhanced-beta operating scenarios, with either broad or peaked profiles to be tested. An even wider operating space is available at reduced current ($q_{95}=5$). In all conditions, the plasma shape must properly conform to tight-fitting internal hardware, as shown in Fig. 4. It must simultaneously be close to the radio-frequency launchers for good wave coupling, close to the outboard conducting structure for effective passive stabilization, and have scrape-off magnetic surfaces terminating only on high-heat-flux divertor targets. While the separatrix always intersects the outboard divertor target at a location close to the pump opening (to maintain particle exhaust), the intersection with the inboard target can move more freely, as explained earlier. The same range of equilibrium flexibility is also available in single-null configurations.

Resistive control coils internal to the vacuum vessel are used in conjunction with both the inboard and outboard passive structure for fast feedback control of the plasma's vertical and radial positions. To control the vertical instability in the presence of system- and plasma-induced noise, the coils and power supplies are designed for random fluctuations in a vertical position with a root-mean-square amplitude of 1 cm and bandwidth equal to the vertical instability growth rate. To maintain good plasma–antenna coupling for continuous

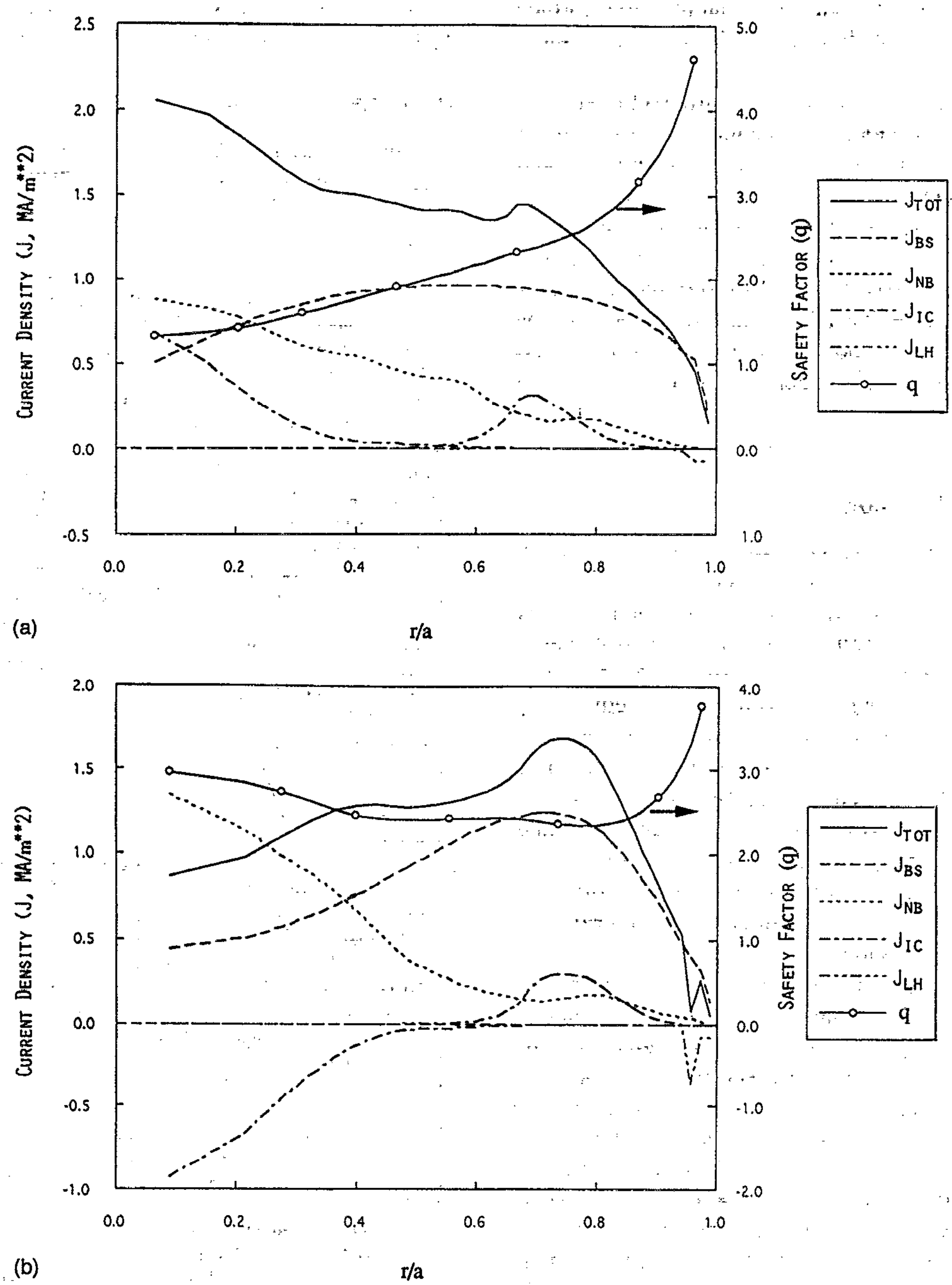

FIG. 5. Profiles of total plasma current, plasma current components, and safety factor for (a) an ARIES-I mode and (b) a reversed-shear mode.

radio-frequency power flow, the coil systems can restore the radial position to nominal in 20 ms (much less than an energy confinement time) following a sudden 20% drop in stored energy. Each coil is divided toroidally into four segments. While these segments will be connected in series initially to perform axisymmetric control functions only, at a later time they can be configured (with the addition of new power supplies) to implement fast feedback control of $n=1$ external modes.

F. Disruption control

Although TPX is designed to structurally withstand disruptions of full-current, high-beta plasmas, disruptions are ultimately incompatible with the goal of reliable steady-state operation, so means to avoid them must be developed. Current profile control will be used as part of the strategy for maintaining configurations with favorable stability properties. Some potentially attractive operating modes also require a close-fitting conducting structure to stabilize nonaxisymmetric MHD instabilities associated with the high-pressure and high edge-current densities. The TPX passive structure includes wide toroidal conductors above and below the outboard midplane (seen in Fig. 4) connected by vertical conductors to provide a path for quasihelical eddy currents needed to stabilize external MHD modes. Preliminary analysis of the TPX structure using a three-dimensional analytical model indicates that it is adequate to stabilize low toroidal mode number deformations in a reversed-shear configuration with β_N up to 5.0.

The passive structure alone may be sufficient to stabilize the external modes, provided they maintain a sufficient toroidal phase velocity with respect to the structure. The tangential, coinjected neutral beams promote such rotation. Motivated by theory[49] and experiments on several machines[50] on the role of field errors in mode locking (which can diminish the effectiveness of passive stabilization), modular external coils are provided on TPX for field-error compensation. Active feedback control of nonaxisymmetric external modes is possible with the modular internal control coils, as described in Sec. IV E.

G. Power and particle control

The TPX plasma-facing components are designed to handle the maximum steady-state heating power of 45 MW. With up to 18 MW, the divertor targets will handle the expected heat load (4–6 MW/m^2), assuming divertor plasma conditions similar to those of present experiments. However, operation at 45 MW will require a factor of 2–3 reduction in the peak divertor heat flux in order to stay safely below the power handling limits (7.5 MW/m^2) of the cooled target structure, since modeling predicts a peak heat flux exceeding 15 MW/m^2, and scaling from experiments suggests values above 10 MW/m^2. The peak heat flux will be reduced by increasing the radiative losses in the edge, scrape-off layer, and divertor plasmas through impurity plus deuterium gas fueling in the divertor region.

Significant heat flux reduction by gas injection has already been demonstrated in a number of divertor tokamaks;[51] neon and argon are expected to be efficient radiators at the low temperatures expected in the divertor region, but poor radiators in the very high-temperature core plasma [$T_e(0)\sim 15$ keV]. In TPX it will be necessary to also maintain good core energy confinement and current drive efficiency (low Z_{eff} and high T_e) in steady state. Recent experiments on DIII-D have shown that, at a given argon puffing rate, the combination of divertor pumping and midplane fueling can reduce core plasma impurity contamination by factors of 3 or more.[52]

Core fueling in TPX will be provided by neutral beam injection (10^{21} atoms/s initially). Pellet injection can be added later for density profile control. Gas injector arrays in the midplane and divertor regions will provide flexibility in supplying fuel and impurities to optimize radiative-divertor conditions. Particle balance experiments[53] in Tore Supra and DIII-D indicate that conditioned walls continuously pump energetic particles and release thermal particles into the scrape-off layer. These are exhausted from the system by pumped limiters (or pumped divertors), enabling the walls to continue pumping. The TPX will use 350 °C bakeout and overnight glow discharge cleaning to precondition the walls, and then continuous divertor pumping to maintain steady-state particle exhaust. The pumping system provides a variable pumping speed up to 88 m^3/s with external cryopumps connected to the divertor region through 16 large-diameter ducts. In addition, turbomolecular pumps with up to 20 m^3/s are available to test helium exhaust scenarios.

ACKNOWLEDGMENTS

This research was supported by the U.S. Department of Energy, Contract No. DE AC02-76-CH03073.

[1]R. W. Conn, F. Najmabadi, and The ARIES Team, in *Plasma Physics and Controlled Nuclear Fusion Research*, Washington, 1990 (International Atomic Energy Agency, Vienna, 1990), Vol. 3, p. 659.

[2]J. D. Galambos, L. J. Perkins, S. Haney, and J. Mandrekas, "Commercial tokamak reactor potential with advanced tokamak operation," accepted for publication in Nucl. Fusion.

[3]J. R. Ferron, L. L. Lao, T. S. Taylor, Y. B. Kim, E. J. Strait, and D. Wroblewski, Phys. Fluids B **5**, 2532 (1993).

[4]M. Hugon, B. Ph. van Milligen, P. Smeulders, L. C. Appel, D. V. Bartlett, D. Boucher, A. W. Edwards, L.-G. Eriksson, C. W. Gowers, T. C. Hender, G. Huysmans, J. J. Jacquinot, P. Kupschus, L. Porte, P. H. Rebut, D. F. H. Start, F. Tibone, B. J. D. Tubbing, M. L. Watkins, and W. Zwingmann, Nucl. Fusion **32**, 33 (1992).

[5]E. J. Strait, T. S. Taylor, A. D. Turnbull, J.R. Ferron, L. L. Lao, B. Rice, O. Sauter, S. J. Thompson, and D. Wroblewski, in *21st European Physical Society Conference on Controlled Fusion and Plasma Physics*, Montpelier, 1994, edited by E. Joffrin, P. Platz, and P. E. Stott (European Physical Society, Petit-Lancy, Switzerland, 1994), Vol. 18B, Part 1, p. 242.

[6]C. Kessel, J. Manickam, G. Rewoldt, and W. M. Tang, Phys. Rev. Lett. **72**, 1212 (1994).

[7] W. M. Nevins, R. J. Goldston, D. N. Hill, S. C. Jardin, S. S. Medley, G. H. Neilson, L. D. Pearlstein, W. A. Peebles, P. A. Politzer, M. Porkolab, J. A. Schmidt, J. C. Sinnis, K. I. Thomassen, M. Ulrickson, and the TPX/SSAT Team, in *Plasma Physics and Controlled Nuclear Fusion Research*, Würzburg, 1992 (International Atomic Energy Agency, Vienna, 1992), Vol. 3, p. 279; K. I. Thomassen, D. B. Batchelor, J. Bialek, P. T. Bonoli, M. S. Chance, R. H. Bulmer, R. J. Goldston, D. N. Hill, S. C. Jardin, C. E. Kessel, J. Manickam, P. K. Mioduszewski, G. H. Neilson, W. M. Nevins, M. Porkolab, and the TPX National Team, *15th International Conference on Plasma Physics and Controlled Nuclear Fusion Research*, Seville, 1994 (International Atomic Energy Agency, Vienna, 1994), Paper IAEA-CN-60/F-1-2; to be published in Nucl. Fusion Suppl. 1995.

[8]H. Ninomiya, T. Aoyagi, M. Azumi, C. A. Chang, T. Fujita, A. Funahasi, S. Ide, Y. Ikeda, Y. Kamada, M. Kikuchi, H. Kishimoto, G. Kurita, M. Kuriyama, N. Miya, M, Nagami, K. Nagashima, O. Naito, K. Nakagawa, S. Nakajima, S. Oguri, T. Ozeki, A. Sakasai, M. Shimada, R. Shimada, K. Shimizu, Y. Takahashi, T. Takizuka, S. Tanaka, N. Toyoshima, M. Uesaka, K. Ushigusa, M. Wakatani, S. Nakagawa, K. Nakashima, and M. Otsuka in Ref. 7, Paper IAEA-CN-60/F-1-I-1, to be published in Nucl. Fusion Suppl. 1995.

[9]R. W. Conn, F. Najmabadi, S. C. Jardin, and the ARIES Team, in Ref. 7, Paper, F-1-I-6, to be published in Nucl. Fusion Suppl. 1995.

[10]E. A. Lazarus, L. L. Lao, T. H. Osborne, T. S. Taylor, A. D. Turnbull, M. S. Chu, A. G. Kellman, E. J. Strait, J. R. Ferron, R. J. Groebner, W. W. Heidbrink, T. Carlstrom, F. J. Helton, C. L. Hsieh, S. Lippmann, D. Schissel, R. Snider, and D. Wroblewski, Phys. Fluids B **4**, 3644 (1992).

[11]V. P. Bhatnagar, A. Taroni, J. J. Ellis, J. Jacquinot, and D. F. H. Start, Plasma Phys. Controlled Nucl. Fusion **31**, 15, 2111 (1989).

[12] *ITER Conceptual Design Report*, ITER Documentation Series No. 18 (International Atomic Energy Agency, Vienna, 1991).

[13]F. Najmabadi, R. W. Conn, and the ARIES Team, *Institute of Electrical and Electronics Engineers*, 13th Symposium on Fusion Engineering, Knoxville, 1989 (Institute of Electrical and Electronics Engineers, New York, 1989), Vol. 2, p. 1021.

[14]M. Kikuchi, Nucl. Fusion **30**, 265 (1991).

[15]T. Ozeki, M. Azumi, S. Tokuda, and S. Ishida, Nucl. Fusion **33**, 1025 (1993); T. Ozeki, M. Azumi, T. Tsunematsu, K. Tani, M. Yagi, and S. Tokuda, in Rev. 7, Würzburg, 1992, Vol. 2, p. 187; J. Manickam, M. S. Chance, S. C. Jardin, C. Kessel, D. Monticello, N. Pomphrey, A. Reiman, C. Wang, and L. E. Zakharov, Phys. Plasmas **1**, 1601 (1994); H. St. John, T. S. Taylor, Y. R. Lin-Liu, and A. D. Turnbull, in Ref. 7, Paper D-P-II-8, to be published in Nucl. Fusion Suppl. 1995.

[16]N. R. Sauthoff, N. Asakura, R. Bell, M. S. Chance, P. Duperrex, J. Faunce, H. Fishman, R. J. Fonck, G. Gammel, G. J. Greene, R. Hatcher, P. J. Heitzenroeder, A. Holland, S. C. Jardin, T. Jiang, R. Kaita, S. M. Kaye, C.

E. Kessel, T. Kozub, H. Kugel, D. Kungl, B. LeBlanc, F. Levinton, J. Manickam, M. Okabayashi, M. Ono, S. F. Paul, E. Powell, Y. Qin, D. R. Roberts, S. Schweitzer, S. Sesnic, and H. Takahashi, in Ref. 1, Vol. 1, p. 709.

[17] E. J. Strait, L. L. Lao, T. S. Taylor, M. S.Chu, J. K. Lee, A. D. Turnbull, S. L. Allen, N. H. Brooks, K. H. Burrell, R. W. Callis, T. N. Carlstrom, M. S. Chance, A. P. Colleraine, D. Content, J. C. DeBoo, J. Ferron, J. M. Greene, R. J. Groebner, W. W. Heidbrink, F. J. Helton, D. N. Hill, R.-M. Hong, N. Hosogane, W. Howl, C. L. Hsieh, G. L. Jackson, G. L. Jahns, A. G. Kellman, J. Kim, S. Kinoshita, E. A. Lazarus, P. J. Lomas, J. L. Luxon, M. A. Mahdavi, Y. Neyatani, T. Ohkawa, T. H. Osborne, D. O. Overskei, T. Ozeki, M. Perry, P. I. Petersen, T. W. Petrie, J. C. Phillips, G. D. Porter, D. P. Schissel, J. T. Scoville, R. P. Seraydarian, M. Shimada, T. C. Simonen, R. T. Snider, R. D. Stambaugh, T. D. Stav, H. St. John, R. E. Stockdale, U. Stroth, and R. Wood, in *Plasma Physics and Controlled Nuclear Fusion Research*, Nice, 1988 (International Atomic Energy Agency, Vienna, 1988), Vol. 1, p. 83.

[18] A. Bondeson and D. J. Ward, Phys. Rev. Lett. **72**, 2709 (1994); N. Pomphrey, S. C. Jardin, J. Bialek, M. S. Chance, D. A. D'Ippolito, J. M. Finn, R. Fitzpatrick, J. L. Johnson, C. E. Kessel, J. Manickam, D. A. Monticello, J. R. Myra, M. Ono, W. Park, A. Reiman, G. Rewoldt, W. M. Tang, E. J. Valeo, and L. E. Zakharov, in Ref. 7, Paper D-1-I-4, to be published in Nucl. Fusion Suppl. 1995.

[19] A. D. Turnbull, T. S. Taylor, E. J. Strait, S. J. Thompson, M. S. Chu, J. R. Ferron, R. J. LaHaye, L. L. Lao, R. T. Snider, B. W. Rice, D. Wroblewski, O. Sauter, M. E. Mauel, A. Popov, N. Popov, D. J. Lightly, and J. D. Williams, Paper, A-5-II-4, to be published in Nucl. Fusion Suppl. 1995.

[20] J. M. Finn, accepted for publication in Phys. Plasmas.

[21] K. Oasa, H. Aikawa, Y. Asahi, K. Hoshino, T. Kawakami, H. Kawashima, H. Maeda, M. Maeno, T. Matsuda, Y. Miura, K. Nagashima, H. Ogawa, T. Ogawa, M. Sasaki, T. Shina, T. Shoji, H. Tamai, K. Uehara, T. Yamauchi, K. Hasegawa, A. Honda, Y. Kashiwa, K. Kikuchi, M. Komata, F. Okano, M. Saitou, E. Sato, N. Seki, T. Shibata, N. Suzuki, T. Tanaka, T. Tani, T. Tokutake, Y. Tomiyama, and K. Umino, in Ref. 7, Paper A3/5-P-15, to be published in Nucl. Fusion Suppl. 1995.

[22] R. Kaita, N. Asakura, S. H. Batha, R. E. Bell, S. Bernabei, L. Blush, R. Cesario, M. S. Chance, T. K. Chu, R. W. Conn, M. Corneliussen, W. Davis, D. A. D'Ippolito, R. Doerner, J. L. Dunlap, A. C. England, H. Fishman, G. Gettelfinger, T. Gibney, N. Greenough, J. H. Harris, R. Hatcher, G. H. Hekel, H. Herrmann, Y. Hirooka, S. P. Hirshman, D. W. Ignat, R. C. Isler, S. C. Jardin, S. Jones, S. M. Kaye, J. Kesner, C. Kessel, T. Kozub, H. Kugel, L. Lagin, B. LeBlanc, D. K. Lee, F. Levinton, S. C. Luckhardt, J. Manickam, M. E. Mauel, G. A. Navratil, M. Okabayashi, H. Oliver, M. Ono, F. Paoletti, S. F. Paul, S. Preische, F. Rimini, P. Roney, N. R. Sauthoff, L. Schmitz, S. Schweitzer, T. Seki, S. Sesnic, Y. Sun, H. Takahashi, W. Tighe, G. Tynann, E. J. Valeo, S. von Goeler, K. Voss, P. Woskov, and A. Zolfaghari, in Ref. 7, Würzburg, 1992, Vol. 1, p. 635.

[23] S. Ide, O. Naito, T. Kondoh, Y. Ikeda, K. Ushigusa, T. Fujita, M. Matsuoka, and the JT-60 Team, in Ref. 7, Paper A-5-I-4, to be published in Nucl. Fusion Suppl. 1995.

[24] C. C. Petty, M. E. Austin, F. W. Baity, R. W. Callis, S. C. Chiu, J. S. DeGrassie, C. B. Forrest, R. L. Freeman, P. Gohil, R. H. Goulding, R. W. Harvey, D. J. Hoffman, H. Ikezi, R. A. James, K. Kupfer, J. H. Lee, Y.-R. Lin-Liu, T. C. Luce, R. I. Pinsker, M. Porkolab, R. Prater, J. P. Squire, and D. W. Swain, in Ref. 7, Paper A3/5-P-6, to be published in Nucl. Fusion Suppl. 1995.

[25] B. Saoutic, A. Bécoulet, G. T. Hoang, T. Hutter, V. Beaumont, J. P. Coulon, E. Joffrin, H. Kuus, and L. Ladurelle, in Ref. 7, Paper A-3-I-6, to be published in Nucl. Fusion Suppl. 1995.

[26] R. Majeski, N. J. Fisch, H. Adler, S. Batha, M. G. Bell, R. Bell, M. Bitter, N. L. Bretz, R. Budny, C. E. Bush, S. Cauffman, Z. Chang, D. Darrow, A. C. England, E. D. Fredrickson, H. P. Furth, G. R. Hanson, M. C. Herrman, K. W. Hill, J. C. Hosea, H. Hsuan, E. F. Jaefer, A. C. Janos, F. C. Jobes, L. C. Johnson, C. F. F. Karney, F. Levinton, E. Mazzucato, S. S. Medley, D. Mikkelsen, D. Mueller, M. Murakami, H. E. Mynick, R. Nazikian, D. K. Owens, H. Park, C. K. Phillips, A. T. Ramsey, D. A. Rasmussen, J. M. Rax, J. H. Rogers, G. Schilling, J. F. Schivell, S. D. Scott, P. Snyder, J. E. Stevens, E. Synakowski, G. Taylor, E. J. Valeo, Z. H. Wang, J. B. Wilgen, J. R. Wilson, K. L. Wong, M. C. Zarnstorff, and S. J. Zweben, in Ref. 7, Paper A-3-I-4, to be published in Nucl. Fusion Suppl. 1995.

[27] C. Gormezano and the JET Team, in Ref. 7, Würzburg, 1992, Vol. I, p. 587.

[28] M. Porkolab, R. Boivin, F. Bombarda, P. Bonoli, C. Christensen, D. Garnier, S. Fairfax, C. Fiore, J. Goetz, S. Golovato, M. Graf, R. Granetz, M. Greenwald, D. Gwinn, S. Horne, T. Hsu, A. Hubbard, I. Hutchinson, J. Irby, D. Jablonski, C. Kurz, B. LaBombard, B. Lipschultz, T. Luke, E. Marmar, M. May, A. Mazurenko, G. McCracken, R. Nachtrieb, A. Niemczewski, P. O'Shea, J. Reardon, J. Rice, J. Schachter, J. Snipes, J. Sorci, P. Stek, Y. Takase, J. Terry, G. Tinios, J. Urbahn, Y. Wang, R. Watterson, B. Welch, and S. Wolfe, in Ref. 7, Paper A-1-II-2, to be published in Nucl. Fusion Suppl. 1995; B. Lipschultz, J. Goetz, B. LaBombard, G. McCracken, J. Terry, D. Jablonski, C. Kurz, A. Niemcsewski, J. Snipes, and the Alcator Group, "Divertor results from the Alcator C-Mod tokamak," to be published in J. Nucl. Mat.

[29] D. N. Hill, S. L. Allen, N. H. Brooks, D. Buchenauer, J. W. Cuthbertson, T. E. Evans, M. E. Fenstermacher, Ph. Ghendrih, D. Hillis, J. T. Hogan, A. W. Hyatt, G. L. Jackson, R. A. James, R. Jong, C. H. Lasnier, A. W. Leonard, M. A. Mahdavi, R. Maingi, M. M. Menon, P. K. Mioduszewski, R. A. Moyer, T. W. Petrie, G. D. Porter, M. E. Rensink, M. J. Schaffer, G. M. Staebler, D. M. Thomas, M. R. Wade, J. G. Watkins, F. Weschenfelder, W. P. West, D. Whyte, and R. Wood, in Ref. 7, Paper A-4-I-2, to be published in Nucl. Fusion Suppl. 1995.

[30] D. L. Hillis, M. R. Wade, J. T. Hogan, M. A. Mahdavi, R. Maingi, W. P. West, N. H. Brooks, K. H. Burrell, D. F. Finkenthal, R. J. Groebner, G. L. Jackson, C. C. Klepper, G. L. Laughon, M. M. Menon, and P. K. Mioduszewski, in Ref. 7, Paper A2/4-P-11, to be published in Nucl. Fusion Suppl. 1995.

[31] J. L. Terry, F. Bombarda, J. A. Goetz, M. A. Graf, C. Kurz, B. LaBombard, B. Lipschultz, E. S. Marmar, G. M. McCracken, J. E. Rice, J. A. Snipes, B. Welch, R. L. Boivin, C. Christensen, S. Fairfax, C. Fiore, S. Golovato, R. S. Granetz, J. Irby, M. J. Greenwald, S. Horne, T. Hsu, A. Hubbard, I. H. Hutchinson, D. Jablonski, T. Luke, M. May, A. Niemczewski, M. Porkolab, J. Schachter, P. Stek, Y. Takese, R.Watterson, and S. Wolfe, in Ref. 7, Paper A-4-I-6, to be published in Nucl. Fusion Suppl. 1995.

[32] D. J. Campbell and the JET Team, in Ref. 7 (International Atomic Energy Agency), Paper, A-4-I-4, to be published in Nucl. Fusion Suppl. 1995.

[33] C. J. Lasnier, D. N. Hill, S. L. Allen, R. A. Jong, A. W. Leonard, T. W. Petrie, and J. G. Watkins, Bull. Am. Phys. Soc. **39**, 1650 (1994).

[34] M. Kaufmann, K. Lackner, V. Mertens, J. Neuhauser, H. Zohm, M. Bessenrodt-Weberpals, K. Büchl, S. Fiedler, A. Field, Ch. Fuchs, C. Garcia-Rosales, O. Gruber, F. Haas, A. Herrmann, W. Herrmann, S. Hirsch, A. Kallenbach, P. Lang, F. Mast, S. C. Pitcher, M. Schittenhelm, J. Stober, W. Suttrop, M. Troppmann, M. Weinlich, in Ref. 7, Paper A-4-I-1, to be published in Nucl. Fusion Suppl. 1995.

[35] P. J. Lomas, and the JET Team, in Ref. 7, Paper A-2-I-4, to be published in Nucl. Fusion Suppl. 1995.

[36] C. Gormezano, and the JET Team, in Ref. 7, Paper A-5-I-3, to be published in Nucl. Fusion Suppl. 1995.

[37] M. Kikuchi and the JT-60 Team, in Ref. 7, Paper A-1-I-2, to be published in Nucl Fusion Suppl. 1995.

[38] X. Garbet, A. Géraud, L. Baylor, H. Capes, J. H. Chatenet, F. Clairet, L. Colas, C. de Michelis, C. Desgranges, J. C. M. de Haas, P. Devynck, G. Gervàis, C. Gil, Ph. Ghendrih, D. Grésillon, A. Grosman, L. Guiziou, P. Hennequin, G. T. Hoang, T. Hutter, E. Joffrin, P. Laporte, C. Laviron, M. Mattioli, M. Paume, J. Payan, A. L. Pecquet, A. Quémeneur, A. Truc, and X. L. Zou, in Ref. 7, Paper A-2-III-4-1/2, to be published in Nucl. Fusion Suppl. 1995.

[39] E. A. Lazarus, A. W. Hyatt, T. H. Osborne, S. E. Attenberger, M. E. Austin, K. H. Nurrell, T. A. Casper, M. S. Chu, J. W. Cuthbertson, E. J. Doyle, P. Gohil, J. M. Greene, C. M. Greenfield, R. J. Groebner, W. A. Houlberg, C.-L. Hsieh, G. L. Jackson, J. Kim, S. Konoshima, L. L. Lao, C. Lasnier, A. W. Leonard, S. I. Lippmann, M. A. Mahdavi, R. Maingi, R. A. Moyer, C. K. Rettig, B. Rice, M. J. Schaffer, D. P. Schissel, R. T. Snider, R. D. Stambaugh, R. E. Stockdale, T. S. Taylor, A. D. Turnbull, M. R. Wade, R. Wood, and D. Wroblewski, in Ref. 7, Paper A-5-I-1, to be published in Nucl. Fusion Suppl. 1995.

[40] R. J. Hawryluk and the TFTR Team, in Ref. 7, Paper A-1-I-1, to be published in Nucl Fusion Suppl. 1995.

[41] R. J. Goldston, S. H. Batha, R. H. Bulmer, D. N. Hill, A. W. Hyatt, S. C. Jardin, F. M. Levinton, S. M. Kaye, C. E. Kessel, E. A. Lazarus, J. Manickam, G. H. Neilson, W. M. Nevins, L. J. Perkins, G. Rewoldt, K. I. Thomassen, M. C. Zarnstorff, and the National TPX Physics Team, Plasma Phys. Controlled Fusion **36**, B213 (1994).

[42] D. N. Hill, B. Braams, J. N. Brooks, D. N. Ruzic, M. Ulrickson, K. A. Werley, R. Campbell, R. J. Goldston, T. Kaiser, G. H. Neilson, P. Mioduszewski, M. E. Rensink, and T. D. Rognlien, *11th International Conference on Plasma Surface Interactions*, Mito, 1994, accepted for publication in J. Nucl. Mat.

[43]D. W. Swain, P. L. Goranson, W. M. Nevins, P. Bonoli, M. Porkolab, A. von Halle, S. Bernabei, and N. Greenough, Fusion Technol. **26**, 361 (1994).
[44]S. S. Medley, Rev. Sci. Instrum. **66**, 297 (1995).
[45]N. A. Uckan, D. E. Post, K. Borrass, J. D. Callen, S. A. Cohen, J. G. Cordey, F. Englemann, N. Fujisawa, M. F. A. Harrison, J. T. Hogan, H. J. Hopman, Y. Igitkhanov, O. Kardaun, S. M. Kaye, S. Krasheninnikov, A. Kukushkin, V. Mukhovatov, W. M. Nevins, A. Nocentini, G. W. Pacher, H. D. Pacher, V. V. Parail, L. D. Pearlstein, L. J. Perkins, S. Putvinskij, K. Riedel, D. J. Sigmar, M. Sugihara, D. W. Swain, T. Takizuka, K. Tani, T. Tsunematsu, N. A. Uckan, J. G. Wegrowe, J. Wesley, S. Yamamoto, R. Yoshino, K. Young, P. N. Yushmanov, and International Contributors, *ITER Physics Design Guidelines: 1989*, ITER Documentation Series No. 10 (International Atomic Energy Agency, Vienna, 1990).
[46]G. R. Harris, "Comparisons of different bootstrap current expressions," submitted to Nucl. Fusion.
[47]G. H. Neilson, D. B. Batchelor, P. K. Mioduszewski, D. J. Strickler, R. J. Goldston, S. C. Jardin, J. M. Bialek, C. E. Kessel, S. S. Medley, J. A. Schmidt, R. H. Bulmer, D. N. Hill, W. M. Nevins, K. I. Thomassen, P. T. Bonoli, M. Porkolab, P. A. Politzer, and P. H. Edmonds, Fusion Technol. **26**, 343 (1994).
[48]K. Tani, M. Azumi, and R. S. Devoto, J. Comput. Phys. **98**, 332 (1992).
[49]R. Fitzpatrick and T. C. Hender, Phys. Fluids B **3**, 644 (1991).
[50]R. J. LaHaye, R. Fitzpatrick, T. C. Hender, A. W. Morris, J. T. Scoville, and T. N. Todd, Phys. Fluids B **4**, 2098 (1992).
[51]T. W. Petrie, D. N. Hill, D. Buchenauer, A. Futch, C. Klepper, S. Lippmann, and M. A. Mahdavi, in *18th European Conference on Controlled Fusion and Plasma Physics*, Berlin, 1991, edited by P. Bachmann and D. C. Robinson (European Physical Society, Petit-Lancy, Switzerland, 1991), Vol. 15C, Part III, p. III-237; D. Stork, A. Tanga, B. Tubbing, and D. Summers, Bull. Am. Phys. Soc. **34**, 2055 (1989); N. Hosogane, Phys. Fluids B **5**, 2417 (1993).
[52]M. J. Schaffer, N. H. Brooks, J. W. Cuthbertson, S. I. Lippmann, M. A. Mahdavi, R. Maingi, M. M. Menon, K. Schaubel, M. R. Wade, and R. D. Wood, Bull. Am. Phys. Soc. **38**, 2058 (1993).
[53]P. K. Mioduszewski, J. T. Hogan, L. W. Owen, R. Maingi, D. K. Lee, D. L. Hillis, C. C. Klepper, M. M. Menon, C. E. Thomas, T. Uckan, M. R. Wade, M. Chatelier, C. Grisolia, Ph. Ghendrih, A. Grosman, T. Hutter, T. Loarer, B. Pégourié, M. A. Mahdavi, and M. Schaffer, , "Experiments on steady state particle control in Tore Supra and DIII-D," in Ref. 42.